European Review for Medical and Pharmacological Sciences 2019; 23: 9965-9977

PPARγ inhibits breast cancer progression by upregulating PTPRF expression

Y.-Y. XU[1], H. LIU[1], L. SU[2], N. XU[1], D.-H. XU[1], H.-Y. LIU[1], D. SPANER[3], Y. BED-DAVID[4,5], Y.-J. LI[1]

[1]Department of Human Anatomy, Basic College of Medical Sciences, Jilin University, Changchun, Jilin, P.R., China
[2]Department of Breast Surgery, China-Japan Union Hospital of Jilin University, Changchun, Jilin, P.R., China
[3]Cellular and Molecular Biology Platform, Sunnybrook Research Institute, Toronto, Ontario, Canada
[4]State Key Laboratory for Functions and Applications of Medicinal Plants, Guizhou Medical University, Guiyang, P.R., China
[5]The Key Laboratory of Chemistry for Natural Products of Guizhou Province and Chinese Academic of Sciences, Guiyang, Guizhou, P.R., China

Abstract. – OBJECTIVE: Peroxisome proliferator-activated receptor γ (PPARγ) regulates fatty acid storage and glucose metabolism. Recently, PPARγ has been reported to be involved in cancer. The present study reported a PPARγ consensus binding site (AGGTCA) in the *ptprf* promoter and identified a strong association between PPARγ and PTPRF expression, as well as their tumor suppressor roles in a v-Ha-Ras-induced model of breast cancer.

MATERIALS AND METHODS: The prognostic potential of PPARγ was assessed with a KM analysis of raw data from 3,951 breast cancer patients. The expression of PPARγ and PTPRF in the rat breast cancer cell lines was detected by Western blot and qPCR. The impact of PPARγ on cancer cell migration, invasion, and growth was confirmed using cell migration assay, transwell cell invasion assay, tri-dimensional soft agar culture, respectively. The binding of PPARγ with the *ptprf* promoter was then examined using electrophoretic mobility shift assay. The inhibitory effect of PPARγ on tumor growth was then examined in mouse tumor model *in vivo*.

RESULTS: It was identified that PPARγ expression is lost in the aggressive v-Ha-Ras-induced breast cancer cell line FE1.2 but highly expressed in less malignant FE1.3 cells. Exogenous expression of PPARγ in FE1.2 cells (FE1.2-PPARγhi) resulted in a marked inhibition of proliferation compared with that in FE1.2-Vector control group. FE1.2-PPARγhi cells also exhibited reduced migration, invasion, and colony formation abilities compared with those of the controls. The PPARγ agonist rosiglitazone also suppressed the malignant properties of FE1.2 cells. Protein tyrosine phosphatase receptor F (PTPRF), a downstream target of PPARγ, was markedly induced in FE1.2-PPARγhi cells. A PPARγ consensus binding site (AGGTCA) was identified in the *ptprf* promoter, and an electrophoretic mobility shift assay confirmed that PPARγ bind to this promoter. Similar to the effect of vector-mediated overexpression of PPARγ, ectopic overexpression of PTPRF in FE1.2 cells led to reduced proliferation. Furthermore, a PPARγ antagonist (GW9662) and PTP inhibitor (NSC87877) abrogated the suppressive function of PPARγ and PTPRF in FE1.2 cells, respectively. PPARγ overexpression or activation suppressed the progression and distant organ metastasis of breast cancer cells in a NOD/SCID mouse model.

CONCLUSIONS: These results suggest that PPARγ inhibits tumor cell proliferation, at least in part, through direct regulation of the ptprf gene and that PPARγ is a potential target for breast cancer treatment.

Key Words:
Peroxisome proliferator-activated receptor γ, Breast cancer suppression, Protein tyrosine phosphatase receptor F, Downstream target, NOD/SCID

Introduction

As one of the most fatal cancer types in females, breast cancer affects ~1 in 10 women worldwide[1]. Despite decades of extensive studies on breast cancer treatment, the survival rate of metastat-

Corresponding Authors: You-Jun Li, MD; e-mail: 15204319988@163.com
Yaacov Ben-David, MD; e-mail: yaacovbendavid@hotmail.com

ic breast cancer patients is low. Identification of genes responsible for mammary tumor resistance and susceptibility may allow for the development of targeted therapies to improve the treatment of this disease[2].

Peroxisome proliferator-activated receptors (PPARs) are a family of essential nuclear receptors that bind directly to specific regions of DNA and regulate the expression of the target genes. There are three types of PPAR (α, β/δ, and γ), among which PPARγ has received most attention due to its implications in the pathology of numerous diseases. PPARγ is highly expressed in adipose tissues and exerts an anti-proliferative effect in pre-adipocytes and possibly other cell types[3]. Activation of PPARγ has a marked impact on tumor cell growth, apoptosis, and differentiation[4]. While in most studies[5], PPARγ was determined to act as a tumor suppressor, others[6] have reported that it promotes tumor growth. Although the mechanisms underlying the oncogenic effects of PPARγ remain largely elusive, it is speculated that PPARγ may influence cellular activities and adjust the cellular environment by specific gene regulation[7,8]. Indeed, PPARγ has been considered a therapeutic target for the treatment of colon[9], lung[10], and breast cancer[11]. The currently available synthetic PPARγ agonists have also proven good safety treatment profiles[12,13], but a better understanding of the biology of PPARg in cancer is required to realize its therapeutic potential.

It has been reported that protein tyrosine phosphatase receptor F (PTPRF) functions as a tumor suppressor gene and inhibits breast cancer growth and metastasis[14]. The present study reported a PPARγ consensus binding site (AGGTCA) in the *ptprf* promoter and identified a strong association between PPARγ and PTPRF expression, as well as their tumor suppressor roles in a v-Ha-Ras-induced model of breast cancer.

Materials and Methods

Bioinformatics Analysis

Kaplan-Meier (KM) plotter (http://kmplot.com/analysis/) was used to determine the prognostic values of PPARγ in breast cancer[15]. A dataset of 3,951 cancer patients with their gene expression data and survival information was downloaded from Gene Expression Omnibus (GEO; https://www.ncbi.nlm.nih.gov/geo/) and divided into high- and low-expression groups by the median value of PPARγ mRNA expression. The log-rank test followed by Cox proportional hazards regression was used to compare these 2 groups, and a KM plot was drawn. From the KM plotter web page, the number of cases, median values of mRNA expression level, hazard ratio, 95% confidence interval, and log-rank *p*-value were extracted.

Cell Culture

The establishment of the rat breast cancer cell lines was performed as described previously[16]. All cell lines were maintained in α-minimum essential medium (α-MEM; Thermo Fisher Scientific, Waltham, MA, USA), supplemented with 10% fetal bovine serum (FBS; Thermo Fisher Scientific, Waltham, MA, USA) and 1 μg/ml 17-β-estradiol (Sigma-Aldrich; Merck KGaA, Darmstadt, Germany). All culture experiments were repeated independently 3 times. To examine growth rates, $1x10^4$ cells per well were seeded on 24-well plates in triplicate and 3 wells were evaluated on each day for 4 consecutive days. PPARγ agonist rosiglitazone (RG), antagonist GW9662, and PTP inhibitor NSC87877 were obtained from Sigma-Aldrich (Merck KGaA, Darmstadt, Germany).

Cell Migration Assay

Cell migration was determined using a wound healing assay as described previously[14]. In brief, $3x10^5$ cells were seeded in each well of a six-well plate. After the cells were attached to the bottom of the plate at 24 h, a linear scratch was generated using a 1,000-μl pipette tip. The cell layers were washed with PBS to remove cell debris, the fresh culture medium was added and supplementation with RG was performed in certain wells. Cell migration was monitored and images were captured after 24 h.

Transwell Cell Invasion Assay

Transwell 24-well chambers (Corning, Corning, NY, USA) were used to monitor cell invasion. The upper side of the filter was covered with Matrigel (Corning, Corning, NY, USA). α-MEM with 10% FBS as chemoattractant was added to the lower chamber. Cells ($1x10^5$ cells in 100 μl α-MEM) were seeded in the upper chamber and incubated at 37°C for 48 h. Cells that had adhered to the lower side of the membrane were then fixed, stained with Coomassie Brilliant Blue (Sigma-Aldrich; Merck KGaA, Darmstadt, Germany), and counted under a dissecting microscope.

Growth of Cells in Soft Agar

To monitor the growth of cells in soft agar, 2 layers of agarose (Sigma-Aldrich; Merck KGaA, Darmstadt, Germany) were used. The bottom layer with 0.5% agarose and the top layer with 0.3% agarose in α-MEM with 10% FBS were set up in 60-mm plates. The top layer contained 5,000 cells in each plate. The plates were incubated at 37°C for 5-7 days and subsequently, the number of colonies consisting of >25 cells was determined.

Western Blot Analysis

Western blot analysis was performed as described previously[17]. In brief, aliquots of total protein extract (20 μg) from cells were loaded and resolved by 10% sodium dodecyl sulfate-polyacrylamide gel electrophoresis (SDS-PAGE). After electrophoresis, proteins were transferred onto polyvinylidene difluoride membranes (PVDF; EMD Millipore, Billerica, MA, USA). Blots were blocked with 10% fat-free dry milk in phosphate-buffered saline (PBS) containing Tween-20 for 1 h at room temperature, then reacted with appropriate primary and secondary antibodies and proteins were detected using enhanced chemiluminescence (ECL; GE Healthcare, Little Chalfont, UK). Primary murine monoclonal antibodies were obtained from the following sources: PPARγ (cat. no. sc-7273) from Santa Cruz Biotechnology (Santa Cruz, CA, USA) used at a dilution of 1:500; PTPRF (cat. no. 610351) from BD Biosciences (Franklin Lakes, NJ, USA) used at a dilution of 1:500 and β-actin (cat. no. A5441) from Sigma-Aldrich (Merck KGaA, Darmstadt, Germany) used at a dilution of 1:50,000. The secondary anti-mouse immunoglobulin G antibodies (cat. no. 7076) were from Cell Signaling Technology (Beverly, MA, USA) diluted at 1:2,000. Densitometry of the immunoblots was performed using ImageJ software [bundled with 64-bit Java for Windows; version 1.8; National Institutes of Health (NIH), Bethesda, MD, USA]. The densitometry value for each sample was normalized against the value for β-actin to obtain the intensities for PPARγ or PTPRF.

RNA Isolation and Synthesis of Complementary (c)DNA

Native FE1.2 cells and FE1.2 cells transfected with various plasmids were harvested and washed once with cold PBS. Total RNA was extracted using the RNeasy kit (Qiagen GmbH, Hilden, Germany) according to the manufacturer's protocol. Total RNA concentrations were measured using a ONE-DROP2000 spectrophotometer (Thermo Fisher Scientific; Waltham, MA, USA) at 260/280 nm. Subsequent cDNA synthesis was performed using the Superscript III First-Strand Synthesis System for Reverse Transcription-quantitative Polymerase Chain Reaction (RT-qPCR; Thermo Fisher Scientific; Waltham, MA, USA) in a 20-μl reaction containing 2 μg total RNA, 20 mM Tris-HCl (pH 8.4), 2.5 mM $MgCl_2$, 5 mM dithiothreitol, 2.5 μm OligodT20, 0.5 mM each of dNTP and 200U Superscript III Reverse Transcriptase. The priming oligonucleotide was annealed to total RNA by incubation at 65°C for 5 min and cooling to 4°C. RT was performed at 50°C for 50 min and cDNA was stored at –20°C until use for real-time qPCR analysis.

Transfection and Infection

Mouse PPARγ full-length cDNA was obtained from Addgene and sub-cloned into a unique *EcoR*I site of the pcDNA-3.1 vector (Ambion; Thermo Fisher Scientific; Waltham, MA, USA). Mouse PTPRF full-length cDNA was a gift from Dr. Yang (Sunnybrook Research Institute, Toronto, ON, Canada)[18,19] and sub-cloned into the *Xho*I and *EcoR*I sites of the retroviral MSCV2.2 plasmid (Agilent Technologies; Santa Clara, CA, USA). Sequences of the constructs were confirmed prior to transfection. Transfection was performed using Lipofectamine 2000 (Invitrogen; Carlsbad, CA, USA) according to the manufacturer's protocol.

Replication-defective viruses were prepared by transfecting the viral plasmids into the helper-free packaging cell line GP+A[20] as described previously[21]. For viral infection, supernatants from the virus-producing cells were used to infect FE1.2 cells seeded at a density of $2x10^6$/60 mm plate (Corning, Corning, NY, USA) at present polybrene (10 μg/ml; Sigma-Aldrich; Merck KGaA, Darmstadt, Germany). After 48 h, cells were selected with neomycin (800 mg/ml; Sigma-Aldrich; Merck KGaA, Darmstadt, Germany). G418-resistant cells were pooled and subjected to subcloning.

QPCR

Real-time qPCR was performed on a DNA engine Option System (MJ Research Inc, Waltham, MA, USA) using SYBR Green as a double-strand DNA-specific binding dye, as previously described[17,18]. PCR was performed for 40 cycles after initial denaturation (95°C, 5 min) with the following parameters: denaturation at 95°C

for 20 s, annealing of primers at 58°C for 20 s and extension at 72°C for 20 s. The relative fold change in RNA expression was calculated using the $2^{-\Delta\Delta Cq}$ method[22]. β-actin was used as an endogenous control for normalization. Rat primer sequences used for qPCR were as follows: PPARγ-sense, 5'CATTTTTCAAGGGTGCCAGT3' and antisense, 5'GAGGCCAGCATGGTGTAGAT3'; PTPRF sense, 5'CAACACAAGTGCCAAGCTGT3' and antisense, 5'AGGGTCCACAGGAAGGAAGT3'. The primer sequence of GAPDH was: β-actin primers: 5′ forward (5′-GTGACGTTGACATCCGTAAAGA-3′) and 3′ reverse (5′-GCCGGACTCATCGTACTCC-3′).

Electrophoretic Mobility Shift Assay (EMSA)

Nuclear extract was isolated from FE1.3 and other cells using a method described in the previous study[23]. Single-stranded oligonucleotides were radioactively [γ-^{32}P] ATP-labeled (Perkin-Elmer, Inc., Waltham, MA, USA) with T4 polynucleotide kinase (New England Biolabs, Ipswich, MA, USA). Single-stranded oligonucleotides were purified using NUCTrap probe purification columns (Agilent Technologies, Inc, Santa Clara, CA, USA), annealed with 2-fold excess cold complimentary oligonucleotides by boiling for 2 min and cooling at room temperature for 1 h. For competition assays, 10-fold and 100-fold excess cold single-stranded oligonucleotides were added to the reaction. PPARγ antibody (cat. no. sc-7273) from Santa Cruz Biotechnology (Santa Cruz, CA, USA) used at a dilution of 1:50 was added to the reaction to visualize the supershifted band. Samples were electrophoresed on a 5% acrylamide gel in 0.5X Tris-borate-ethylene diamine tetraacetic acid (EDTA) buffer. The gel was dried in a vacuum for 1 h at 80°C and visualized using autoradiography by X-ray film (Life Technologies; Thermo Fisher Scientific; Waltham, MA, USA). The sequence of the 80-bp oligonucleotide containing the peroxisome proliferator response element (PPRE) AGGTCA of the *ptprf* promoter region is CACTGGACACGGTGGCACGTGCATTTGAATTTGACATGAGGTCAGTGAAGTTCAAATGCAAGTGGATGGTTTCAGGGTGG and also used for [γ-^{32}P] ATP-labelled (hot). For cold complementary oligonucleotides, the following sequence was used: CCACCCTGAAACCATCCACTTGCATTTGAACTTCACTGACCTCATGTCAAATTCAAATGCACGTGCCACCGTGTCCAGTG.

Mouse Tumor Model

A total of 15 female NOD/SCID mice were randomly divided into 3 groups, FE1.2-Vector, FE1.2-Vector treated with RG and FE1.2-PPARγ^{hi}. Cells (1×10^6) were injected into the right side, fourth mammary nipple fat pad. After 21 days of incubation, mice were sacrificed, and the breast tumors and lungs were removed and measured, and their images were captured. The tumor volume (V) was calculated according to the formula $V=LxW^2/2$, where L is the length and W is the width. Lungs were fixed with 10% formaldehyde (Sigma-Aldrich; Merck KGaA, Darmstadt, Germany), paraffin-embedded, and sliced. Slices were then stained using the H&E staining method (Sigma-Aldrich; Merck KGaA, Darmstadt, Germany). The lung metastatic colonies were counted using 3 different slices from each mouse and data from 5 independent mice were plotted. All experimental procedures complied with the requirements and approval of the Animal Ethics Committee of Jilin University for laboratory use (Changchun, China; permit no. 2018-52). All procedures were in accordance with the Guide for the Care and the Use of Laboratory Animals manual published by the US National Institute of Health (NIH).

Statistical Analysis

All *in vitro* experiments were performed in triplicate and repeated independently three times. Determination of the ratio of the protein band intensities relative to β-actin, the quantification of colonies in the soft agar growth and migration assays, and cell invasion in the transwell assay was performed for each sample using ImageJ software (NIH). Values are expressed as the mean ± standard error unless otherwise indicated. An unpaired two-tailed Student's *t*-test or analysis of variance (ANOVA) were used to determine the *p*-values for differences between samples. $p<0.05$ was considered a statistical significance.

Results

Differential Expression of PPARγ in Breast Cancer Cells

The prognostic potential of PPARγ was first assessed with a KM analysis of raw data from 3,951 breast cancer patients (Figure 1A). These patients were divided into two groups of high and low PPARγ expression with the cut-off set as the median level. Patients with high levels of PPARγ

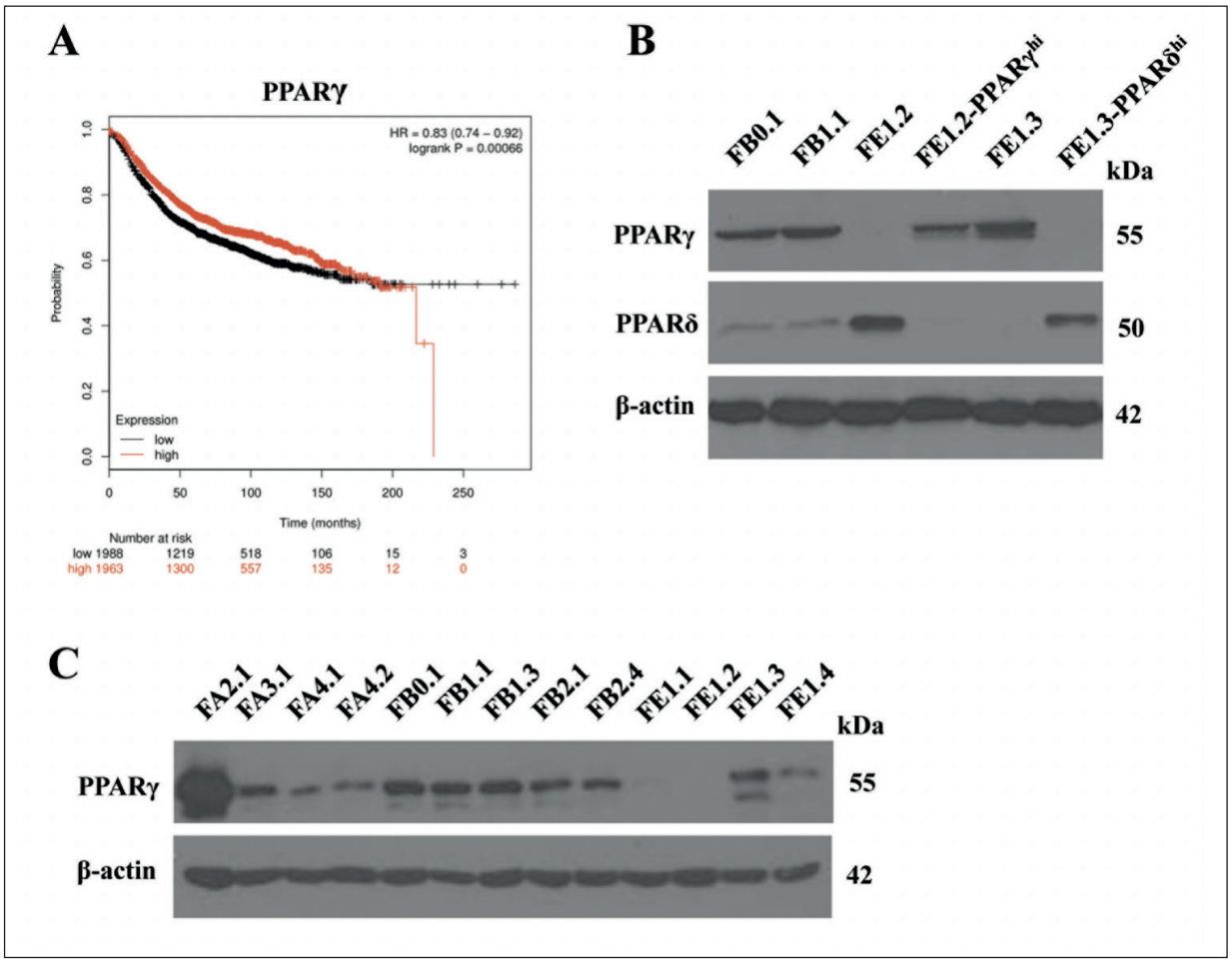

Figure 1. Differential expression of PPARγ in breast cancer cells. **A,** Kaplan-Meier plot of survival rates of breast cancer patients with high and low expression of PPARγ. Log-rank *p*-values and HR (95% confidence interval in parentheses) are provided. **B,** Western blot of PPARγ and PPARδ expression in FE1.3, FE1.2-Vector, FE1.2-PPARγ^{hi}, and FE1.3-PPARδ^{hi} cells. **C,** PPARγ expression in clones of the indicated v-Ha-Ras-induced rat mammary breast cancer cell lines with β-actin as a loading control. HR, hazard ratio; PPAR, peroxisome proliferator-activated receptor.

expression had a noticeably higher survival rate than those with low PPARγ expression. According to this analysis, the level of PPARγ expression is clearly predictive of cancer development and progression.

The mammary carcinoma cell lines were obtained by injecting a v-Ha-Ras-containing retrovirus into the mammary ducts of rats, as described previously[16]. Cell lines with epithelial morphology (FE1.3) and more elongated mesenchymal morphology (FE1.2) were grown along with eleven other cell lines derived from similar virally infected v-Ha-Ras-induced mammary tumors[16]. Measurement of PPARγ expression by Western blot indicated a higher PPARγ expression in FE1.3 compared with that in FE1.2 cells (Figure 1B).

Wang et al[24] have indicated that PPARδ upregulation is positively associated with more aggressive behavior of cancer cells. Comparative analysis of PPARγ to PPARδ in selected cell lines indicated a differential expression pattern in these proteins (Figure 1B). FE1.2 and FE1.3 cells exhibited exclusive expression of either PPARγ or PPARδ, respectively. Of note, after transfection of PPARγ into FE1.2 cells, PPARδ expression disappeared. *Vice versa*, when FE1.3 cells were transfected with PPARδ, PPARγ expression disappeared and PPARδ appeared as the only band on the gel. This complementary pattern suggests an inter-regulatory association between expression of PPARγ and PPARδ in breast cancer cells, as previously described[25].

The expression of PPARγ in all 13 v-Ha-Ras-induced rat breast cancer cell lines was further examined, except for FE1.2, FE1.1 cells also lost PPARγ expression (Figure 1C). Of note, FE1.1 and FE1.2 have the same morphology in cell culture and the same level of expression of PPARδ, as reported in a previous study by our group[24]. All other clones exhibited expression of PPARγ at various levels (Figure 1C).

Ectopic PPARγ Expression Inhibits Breast Cancer Cell Proliferation

To evaluate the influence of PPARγ expression on FE1.2 cells, a series of experiments were performed to measure cell proliferation, migration, and invasion *in vitro*. In growth rate studies (Figure 2A), FE1.2-PPARγ^{hi} cells exhibited a significant delay in proliferation when compared to FE1.2-Vector cells. Indeed, on day 4, the number of cells in control group was ~4 times that in FE1.2-PPARγ^{hi} cells. In addition, the PPARγ agonist RG significantly inhibited the growth of FE1.2 cells, but not as efficiently as transfection with PPARγ overexpression vector.

The result of the wound repair assay revealed that the FE1.2-Vector cells exhibited a higher migratory capacity compared with that of FE1.2-PPARγ^{hi} cells (Figure 2B). The migration rate was 50% lower in FE1.2-PPARγ^{hi} cells than that in control group. In line with this, in the cell invasion experiments, FE1.2-Vector cells exhibited a higher degree of invasion compared with that in the FE1.2-PPARγ^{hi} cells (Figure 2C and D). FE1.2-PPARγ^{hi} cells exhibited a ~60% reduction of invasion compared with that in FE1.2-Vector group (Figure 2D).

The impact of PPARγ on cancer cell growth was further confirmed using tri-dimensional soft agar culture (Figure 2E). After incubation with agarose for 5-7 days, the control FE1.2-Vector cells gave rise to large colonies on the plates. Addition of the PPARg agonist to FE1.2-Vector cells led to a significant reduction in the number and size of colonies. In FE1.2-PPARγ^{hi} group, the number of colonies was reduced by 30%, and in the FE1.2-PPARγ^{hi} group, the number of colonies was reduced by ~70% when compared to the control vector alone cells (Figure 2F). These results suggest that activation of PPARγ in FE1.2 cells suppresses migration, invasion, and colony formation in addition to proliferation.

Regulation of PTPRF Expression by PPARγ in Breast Cancer Cells

The protein tyrosine phosphatase (PTP) family PTPRF is known to be associated with cell invasion, migration, and metastasis in breast cancer[19,20,26], and PTPRF expression is considered a predictive marker in prostate cancer treatment[27]. Given similar properties of PPARg in breast cancer, the present study hypothesized the existence of a close correlation between these two proteins. As indicated by RT-qPCR, FE1.2, and FE1.2-Vector cells express a low level of *ptprf* mRNA (Figure 3A). In FE1.3 cells, high PPARγ expression was associated with high levels of PTPRF (Figure 3A and B). FE1.2-PPARγ^{hi} cells had a ~6-fold higher PTPRF expression than FE1.2-Vector control cells (Figure 3A and B). These data support the notion that PPARγ may directly regulate PTPRF.

To explore the involvement of PTPRF in regulating cell proliferation, the ptprf gene was transduced into FE1.2 cells. High expression of PTPRF was detected in pooled transfected cells (FE1.2-PTPRF^{hi}) when compared with that in FE1.3 and FE1.2-Vector cells (Figure 3C). PTPRF expression in FE1.2 was associated with significantly decreased proliferation when compared with that in the control cells (Figure 3D). This result may suggest that PPARγ exerts its anti-proliferative activity at least in part through the up-regulation of PTPRF.

PPARγ Binds to the ptprf Gene and Regulates its Expression

Regulation of PTPRF by PPARγ may occur by binding to the promoter region. Previous studies[28,29] identified a consensus sequence PPRE or PPARγ consensus binding site. A peroxisome proliferator responsive element (PPRE) was identified in the *ptprf* promoter region, containing a repetitive sequence AGGTCA as a binding site. The mechanism associated with PPARγ-regulated expression of *ptprf* was then examined using EMSA (Figure 4A). As a probe, an oligonucleotide with 80 bp identical to the PPRE (AGGTCA) on the *ptprf* promoter region was synthesized. Nuclear extracts were incubated with [γ-^{32}P] ATP-labeled oligonucleotide and subjected to EMSA. As expected, PPARγ-negative FE1.2 cells and FE1.3 cells treated with an excess of cold oligonucleotide exhibited no bands when compared with FE1.3, FB0.1, and FB1.1cells, which exhibited PPARγ 1 and PPARγ 2 bands. Addition of PPARγ antibodies produced a mobile band (supershift) in FE1.3 cells. This

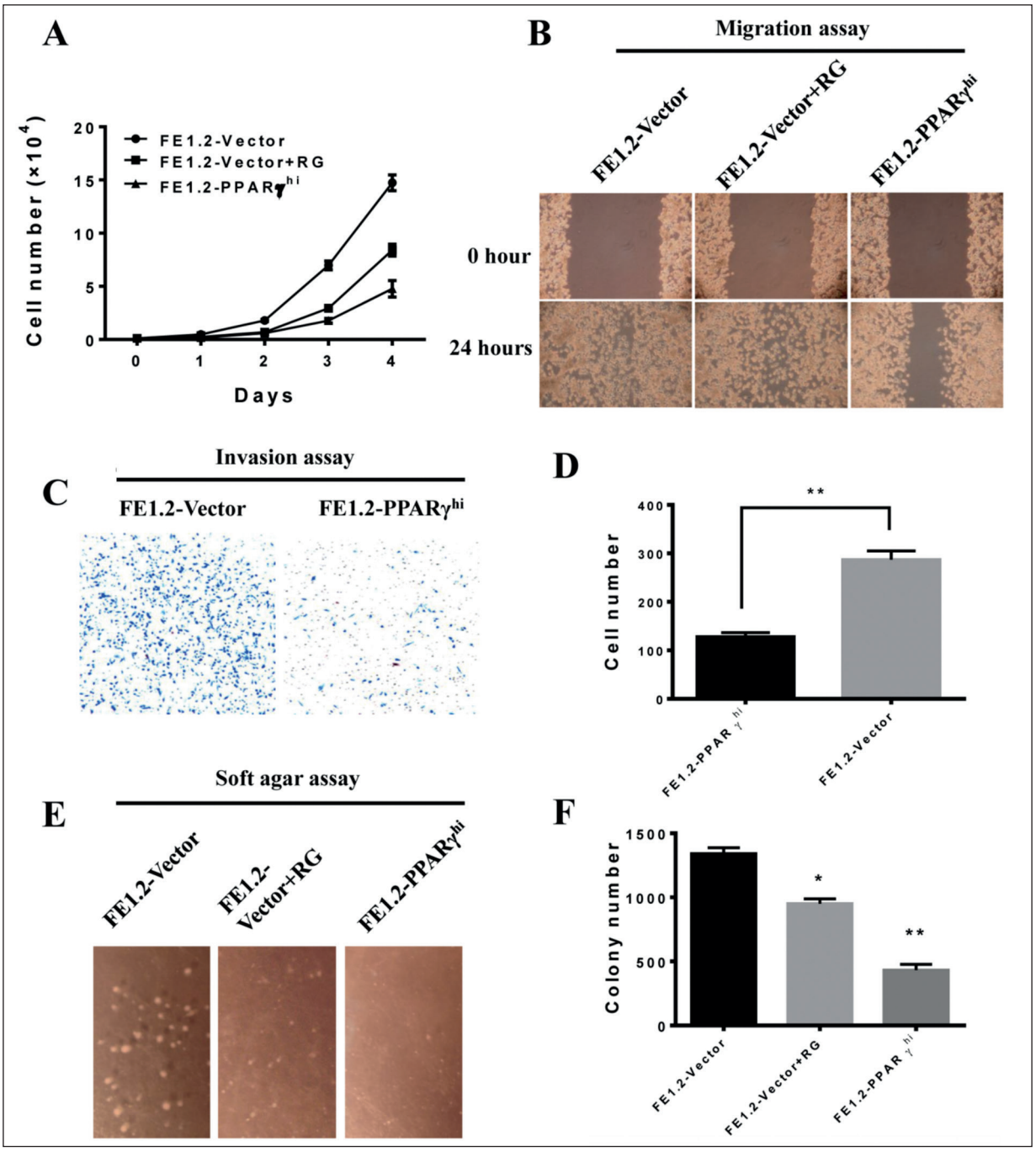

Figure 2. Ectopic PPARγ expression inhibits breast cancer cell proliferation. Behavior of FE1.2 cells after transfection with PPARγ. **A,** Growth rates of FE1.2-Vector, FE1.2-Vector+RG and FE1.2-PPARγ^{hi} cells. **B,** Visual assessment of migratory rates of FE1.2-Vector, FE1.2-Vector+RG and FE1.2-PPARγ^{hi} cells on tissue culture plates (magnification, ×20). (**C**-**D**), Transwell cell invasion assay. **C,** Images (magnification, ×10) of FE1.2-Vector and FE1.2-PPARγ^{hi} cells and **D,** quantified number of migrated cells. **E, F** Soft agar growth assay. **E,** Direct visualization of colony grown on agar from FE1.2-Vector, FE1.2-Vector+RG, and FE1.2-PPARγ^{hi} cells (magnification, ×10). **F,** Colonies of >25 cells were counted and plotted. $^{*}p < 0.05$; $^{**}p < 0.005$; $^{***}p < 0.001$. PPAR, peroxisome proliferator-activated receptor; RG, rosiglitazone.

result supports the hypothesis that PPARγ specifically binds to the promoter region (PPRE) of *ptprf* and regulates its expression.

To further examine the tumor suppressor activity of PPARγ, the PPARγ antagonist GW9662 (10 μM) or the PTP inhibitor NSC87877 (10 μM)

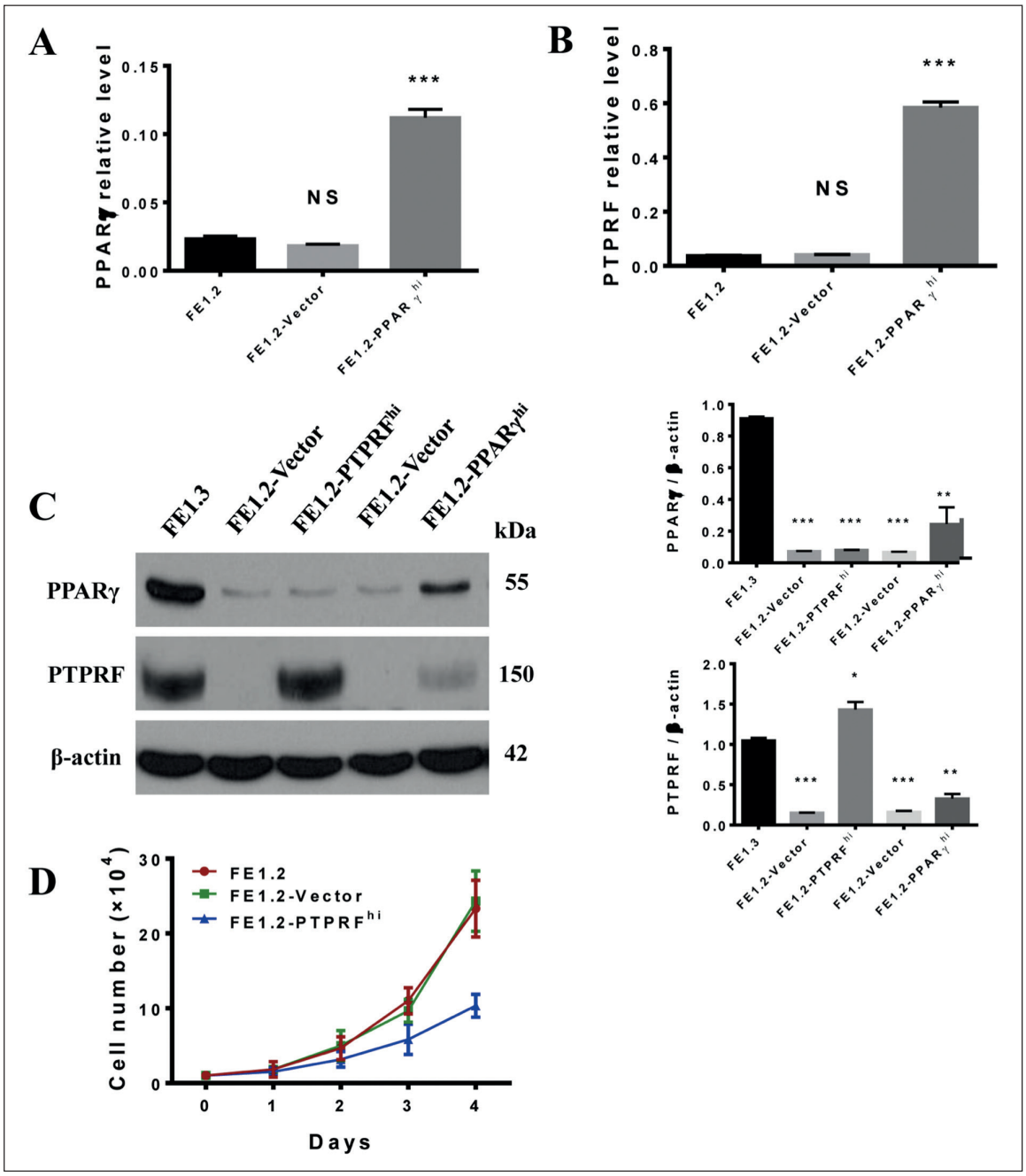

Figure 3. Regulation of PTPRF expression by PPARγ in breast cancer cells. **A, B,** Expression of **A,** PPARγ and **B,** PTPRF in FE1.2, FE1.2-Vector, and FE1.2-PTPRF^{hi} cells determined by reverse transcription-quantitative polymerase chain reaction. **C,** Western blot analysis of the expression of PPARγ and PTPRF in FE1.2 cells transfected with PPARγ and PTPRF expression vectors. FE1.3- and FE1.2-Vector cells were used as controls. The band density of the blots relative to β-actin was quantified by densitometry and presented as graphs in the right panels. **D,** Growth rate of FE1.2-PTPRF^{hi} in comparison to FE1.2 and FE1.2-Vector cells. *$p < 0.05$; **$p < 0.005$; ***$p < 0.001$. NS, not significant; PPAR, peroxisome proliferator-activated receptor.

were added to cultures and the number of cells was determined daily over 4 consecutive days. PPARγ^{hi} cells grew much faster in the presence of GW9662 and NSC87877 (Figure 4B). Treatment with NSC87877, but not with GW9662, made FE1.2 cells overcome the growth inhibitory effect PTPRF overexpression when compared to FE1.2-Vector cells (Figure 4C). The expression levels of PTPRF in FE1.2-PPARγ^{hi} cells were lowered by treatment with GW9662

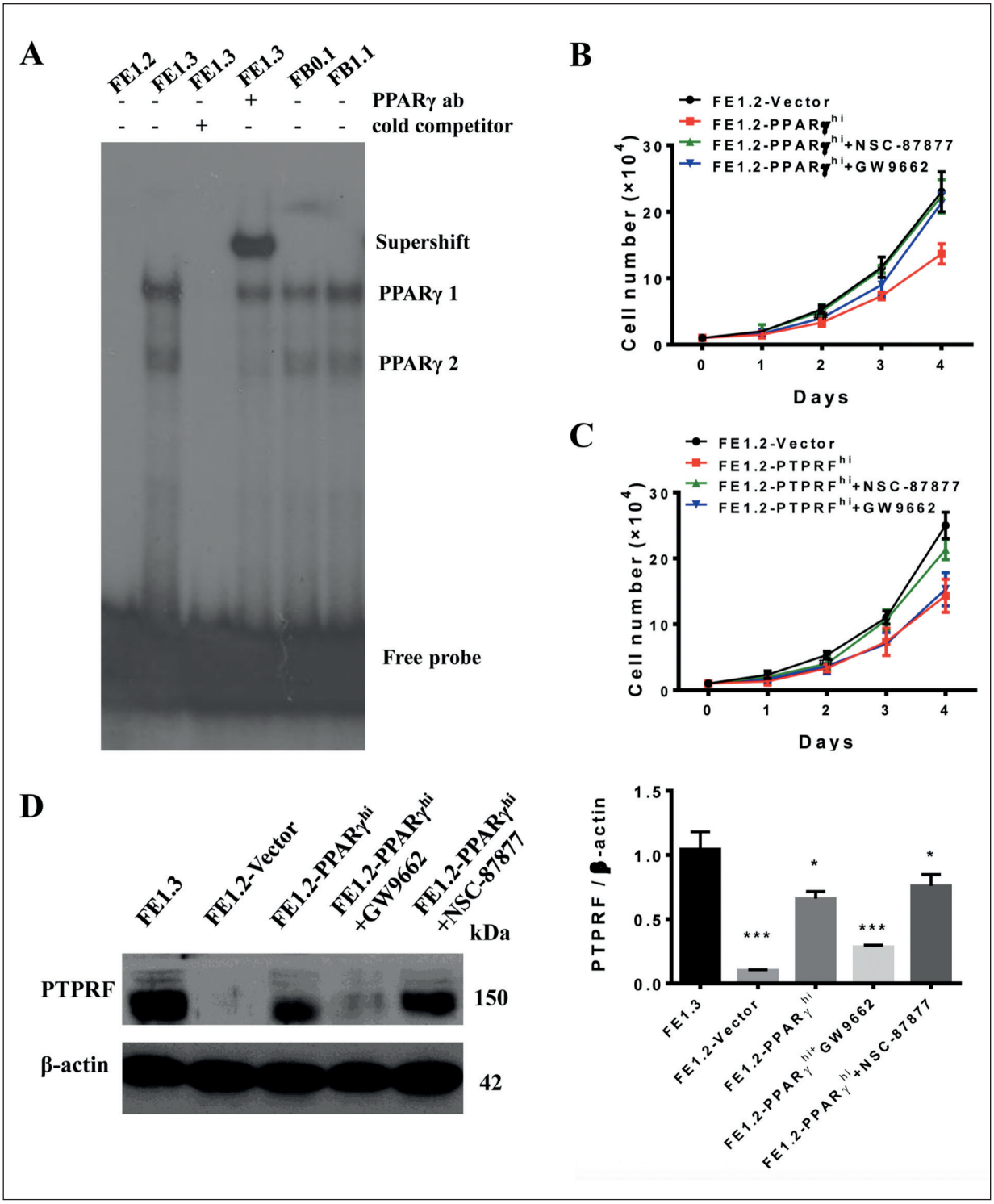

Figure 4. PPARγ binds to the ptprf gene and regulates its expression. **A,** Nuclear extracts from the indicated cells were incubated with [γ-^{32}P]-labelled oligonucleotides containing a PPRE binding site and subjected to an electrophoretic mobility shift assay. For the competition, excessive cold single-stranded oligonucleotides (10- and 100-fold) were added to certain reactions. PPARγ antibody was added to generate supershift. **B, C,** Growth suppression ability of PPARγ and PTPRF was reversed by addition of (**B**) PPARγ antagonist and **C,** PTP inhibitor to the growing culture of the indicated cells. **D,** Western blot analysis revealed that only GW9662, but not NSC87877 treatment blocks PPARγ expression in FE1.2-PPARγ^{hi} cells. *p < 0.05; ***p < 0.001. PPAR, peroxisome proliferator-activated receptor; PTPRF, protein tyrosine phosphatase receptor F; PPRE, peroxisome proliferator response element.

but not NSC87877 (Figure 4D). This result was consistent with the notion that PPARγ suppresses breast cancer growth through the upregulation of PTPRF.

Ectopic Expression of PPARγ in Breast Cancer Cells Inhibits Tumor Growth in NOD/SCID Mice

As PPARγ overexpression in FE1.2 cells suppressed proliferation and invasion *in vitro*, this inhibitory effect was examined *in vivo*. Two groups of female NOD/SCID mice were injected into the nipple fat pad with FE1.2-Vector or FE1.2-PPARγ^{hi} cells (n=5 per group). The third group (5 mice) was injected with FE1-2-Vector cells and subsequently treated with PPARγ agonist RG (1 mg/kg) every other day for two weeks. The mice were sacrificed at day 21, mammary tumors and lungs were removed, their dimensions were measured, and images were captured. The tumor volume in the RG-treated FE1.2-Vector group was reduced by ~30% when compared with that in FE1.2-Vector-injected control group (Figure 5B). The tumor volume in the FE1.2-PPARγ^{hi} group exhibited a greater reduction than that in the RG-treated FE1.2-Vector, namely by ~60% compared with that in FE1.2-Vector group (Figure 5B).

Metastatic lung colonies were also measured. In FE1.2-PPARγ^{hi} group, the number of lung metastatic colonies and their sizes were significantly lower than those in FE1.2-Vector control group (Figure 5C and D). In the FE1.2-Vector with RG treatment group, the number of lung metastatic colonies was also slightly lower than that in FE1.2-Vector group (Figure 5C and D). This result indicates that PPARγ not only suppressed primary tumor growth but also reduced distant organ metastasis by inhibiting cell migration and invasion.

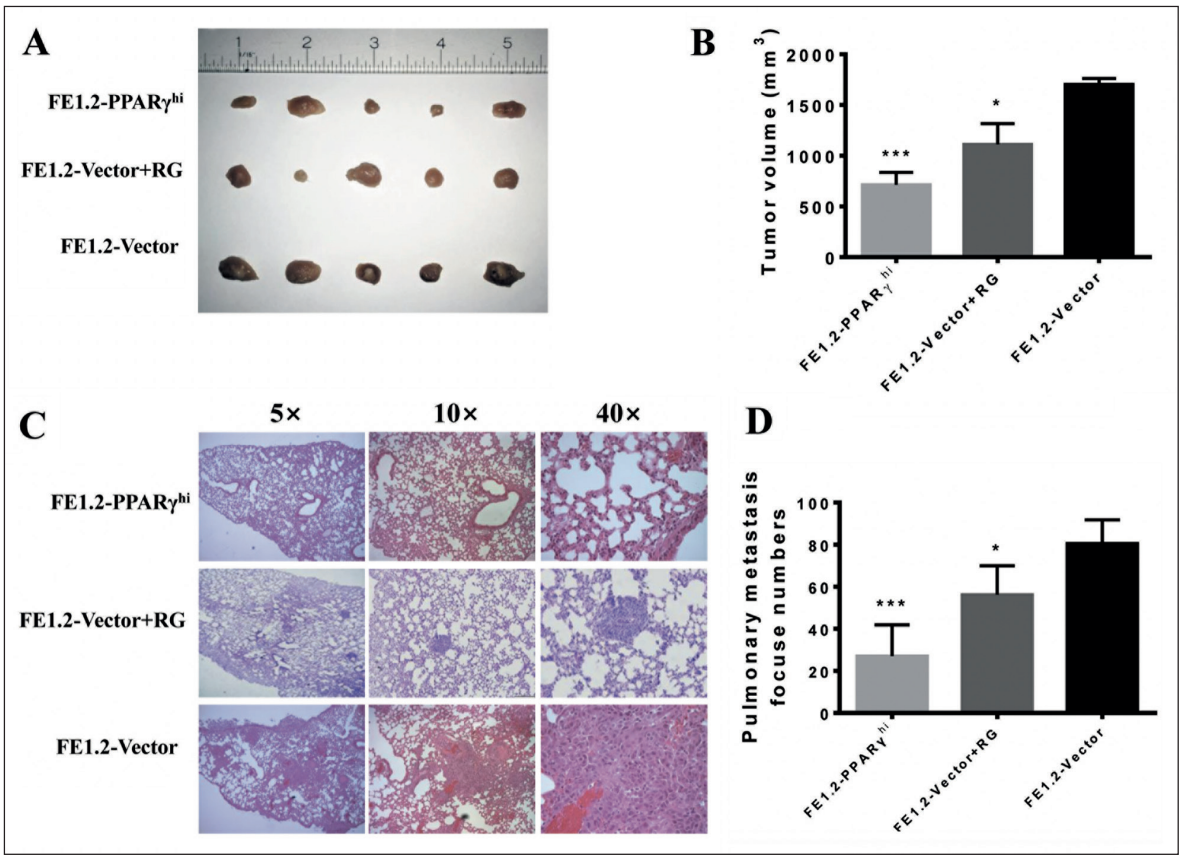

Figure 5. PPARγ expression in breast cancer cells inhibits tumor growth in NOD/SCID mice. **A,** Tumor size and **B,** tumor volume in groups of NOD/SCID mice injected with FE1.2-Vector, FE1.2-PPARγ^{hi} cells or FE1.2-Vector treated with RG (n=5 per group). **C,** Images of lung metastatic colonies of mice injected with FE1.2-PPARγ^{hi}, FE1.2-Vector treated with RG or FE1.2-Vector cells. **D,** Number of lung metastatic colonies from FE1.2-PPARγ^{hi}, FE1.2-Vector treated with RG and FE1.2-Vector injected cells. $^{*}p < 0.05$; $^{***}p < 0.001$. PPAR, peroxisome proliferator-activated receptor; RG, rosiglitazone.

Discussion

The results of the present study further show that PPARγ acts as a tumor suppressor and has a key role in carcinogenesis. PPARγ was demonstrated to suppress cancer cell growth, migration, and invasion through the direct regulation of PTPRF. The results reinforce the notion of a positive association between PPARγ and PTPRF that may be used as a prognostic marker in breast cancer diagnosis and treatment.

A noteworthy observation of the present study and others[30] is the negative effect of PPARγ expression on PPARδ. This result is consistent with the current view that the DNA binding domains for three PPAR subtypes (α, δ, and γ) are 80% identical[31]. Indeed, Wang et al[24] by our group indicated the role of PPARδ as a pro-survival gene in breast cancer cells. Although the role of PPARδ in cancer cell progression remains to be fully elucidated, it is reasonable to speculate that the tumor-suppressor effect of PPARγ may also in part be a result of PPARδ suppression, a notion that remains to be investigated in future studies.

PPARγ is considered a promising molecular target for certain cancer types. Upregulation of PPARγ affects the expression of genes that regulate cell proliferation and apoptosis[32,33]. Accordingly, PPARγ ligands have been demonstrated to inhibit cell proliferation, and to induce cell differentiation and apoptosis. Certain PPARγ ligands, including the thiazolidine family[34], have been reported to have a significant inhibitory effect on cancer cells. While these results suggest that PPARγ is a tumor-suppressor gene, Tachibana et al[35] also indicated that PPARγ enhanced tumor growth under certain circumstances. In the *in vivo* experiment of the present study, overexpression of PPARγ in breast cancer cells was more effective at suppressing tumor growth than treating these cells with agonists. Thus, it is possible that PPARγ ligands and agonists may control overlapping and/or independent functions, a notion that requires to be examined in future studies.

To the best of our knowledge, the present research was the first to demonstrate that PPARγ regulates the expression of PTPRF. It is commonly accepted that PTPRs act as tumor suppressors[36,37]. Overexpression of PTPRF was reported to suppress the WNT pathway by inhibiting β-catenin phosphorylation, and to reduce epithelial cell migration and inhibit tumor formation in nude mice[38]. Downregulation of PTPRF has been reported in liver, gastric, and colorectal cancer[39]. Due to its extracellular domain and regulation of β-catenin signaling, PTPRF may be used as a biomarker in certain cancer types[27].

One of the mechanisms of PTPR dysregulation in cancer is hypermethylation of its promoter[26,40,41], which leads to inactivation of PTPR. As another mechanism, the present data indicated that enforced PPARγ expression also induced PTPRF expression, while PTPRF in FE1.2 cells had no effect on PPARg expression. This one-way stimulation of PTPRF indicates that PPARγ-induced PTPRF expression may subsequently suppress cell proliferation. Thus, the combination of PPARγ and PTPRF may be used as a novel prognostic tool in cancer research.

Conclusions

Overall, the present study confirms that PPARγ functions as a tumor suppressor in breast carcinoma and possibly other cancer types. PPARγ expression directly regulates ptprf, and these two factors are associated with tumor suppressor activity. Whether PPARγ suppresses tumor growth by upregulating ptprf alone or also through regulation of other downstream factors remains to be determined. Development of small molecules that activate PPARγ and PTPRF should provide an important tool for the treatment of breast and other cancer types.

Conflict of Interest

The Authors declare that they have no conflict of interests.

Acknowledgements

The authors would like to thank Dr Yang (Sunnybrook Research Institute, Toronto, ON, Canada) for gifting the PTPRF plasmid. This investigation was supported by the Research Grant from the National Natural Science Foundation of China (Grant no. 81372456 to Y-J L).

Authors' Contribution

Y-YX initiated the experiment, analyzed data, and wrote the manuscript. HL, LS, NX, DHX, and H-YL provided support with experimental techniques. DS also contributed to manuscript writing and revision. Y-BD and Y-JL conceived the project and supervised all experiments. All authors have read and approved the final manuscript.

References

1) Klein G. Toward a genetics of cancer resistance. Proc Natl Acad Sci U S A 2009; 106: 859-863.
2) Lee KM, Giltnane JM, Balko JM, Schwarz LJ, Guerrero-Zotano AL, Hutchinson KE, Nixon MJ, Estrada MV, Sánchez V, Sanders ME, Lee T, Gómez H, Lluch A, Pérez-Fidalgo JA, Wolf MM, Andrejeva G, Rathmell JC, Fesik SW, Arteaga CL. MYC and MCL1 cooperatively promote chemotherapy-resistant breast cancer stem cells via regulation of mitochondrial oxidative phosphorylation. Cell Metab 2017; 26: 633-647.
3) Spiegelman BM. PPAR-gamma: adipogenic regulator and thiazolidinedione receptor. Diabetes 1998; 47: 507-514.
4) Koeffler HP. Peroxisome proliferator-activated receptor γ and cancers. Clin Cancer Res 2003; 9: 1-9.
5) Krishnan A, Nair SA, Pillai MR. Biology of PPAR gamma in cancer: a critical review on existing lacunae. Curr Mol Med 2007; 7: 532-540.
6) Saez E, Tontonoz P, Nelson MC, Alvarez JG, Ming UT, Baird SM, Thomazy VA, Evans RM. Activators of the nuclear receptor PPARgamma enhance colon polyp formation. Nat Med 1998; 4: 1058-1061.
7) Kaul D, Anand PK. Regulation of PPAR-gamma gene in human promyelocytic HL-60 cell line. Leuk Res 2003; 27: 683-686.
8) Ren R, Chen Z, Zhao X, Sun T, Zhang Y, Chen J, Lu S, Ma W. A possible regulatory link between Twist 1 and PPARγ gene regulation in 3T3-L1 adipocytes. Lipids Health Dis 2016; 15: 189.
9) Campbell SE, Stone WL, Whaley SG, Qui M, Krishnan K. Gamma (γ) tocopherol upregulates peroxisome proliferator-activated receptor (PPAR) gamma (γ) expression in SW 480 human colon cancer cell lines. BMC Cancer 2003; 3: 25.
10) Wick M, Hurteau G, Dessev C, Chan D, Geraci MW, Winn RA, Heasley LE, Nemenoff RA. Peroxisome proliferator-activated receptor-γ is a target of nonsteroidal anti-Inflammatory drugs mediating cyclooxygenase-independent inhibition of lung cancer cell growth. Mol Pharmacol 2002; 62: 1207-1214.
11) Suh N, Wang Y, Williams CR, Risingsong R, Gilmer T, Willson TM, Sporn MB. A new ligand for the peroxisome proliferator-activated receptor-γ(PPAR-γ), GW7845, inhibits rat mammary carcinogenesis. Cancer Res 1999; 59: 5671-5673.
12) Wu XJ, Sun XH, Wang SW, Chen JL, Bi YH, Jiang DX. Mifepristone alleviates cerebral ischemia-reperfusion injury in rats by stimulating PPARγ. Eur Rev Med Pharmacol Sci 2018; 22: 5638-5696.
13) Vetuschi A, Pompili S, Gaudio E, Latella G, Sferra R. PPAR-γ with its anti-inflammatory and anti-fibrotic action could be an effective therapeutic target in IBD. Eur Rev Med Pharmacol Sci 2018; 22: 8839-8848.
14) Rutnam ZJ, Yang BB. The non-coding 3' UTR of CD44 induces metastasis by regulating extracellular matrix functions. J Cell Sci 2012; 125: 2075-2085.
15) Gyorffy B, Lanczky A, Eklund AC, Denkert C, Budczies J, Li Q, Szallasi Z. An online survival analysis tool to rapidly assess the effect of 22,277genes on breast cancer prognosis using microarray data of 1,809 patients. Breast Cancer Res Treat 2010; 123: 725-731.
16) Li YJ, Song R, Korkola JE, Archer MC, Ben-David Y. Cyclin D1 is necessary but not sufficient for anchorage-independent growth of rat mammary tumor cells and is associated with resistance of the Copenhagen rat to mammary carcinogenesis. Oncogene 2003; 22: 3452-3462.
17) Li YJ, Liu G, Li Y, Vecchiarelli-Federico LM, Liu JC, Zacksenhaus E, Shan SW, Yang BB, Li Q, Dash R, Fisher PB, Archer MC, Ben-David Y. mda-7/IL-24 Expression inhibits breast cancer through upregulation of growth arrest-specific gene 3 (gas3) and disruption of β1 integrin function. Mol Cancer Res 2013; 11: 593-603.
18) Du WW, Fang L, Li M, Yang X, Liang Y, Peng C, Qian W, O'Malley YQ, Askeland RW, Sugg SL, Qian J, Lin J, Jiang Z, Yee AJ, Sefton M, Deng Z, Shan SW, Wang CH, Yang BB. MicroRNA miR-24 enhances tumor invasion and metastasis by targeting PTPN9 and PTPRF to promote EGF signaling. J Cell Sci 2013; 126: 1440-1453.
19) Yang T, Zhang JS, Massa SM, Han X, Longo FM. Leukocyte common antigen-related tyrosine phosphatase receptor: increased expression and neuronal-type splicing in breast cancer cells and tissue. Mol Carcinog 1996; 25: 139-149.
20) Markowitz D, Goff S, Bank A. A safe packaging line for gene transfer: separating viral genes on two different plasmids. J Virol 1988; 62:1120-1124.
21) Bani MR, Rak J, Adachi D, Wiltshire R, Trent JM, Kerbel RS, Ben-David Y. Multiple features of advanced melanoma recapitulated in tumorigenic variants of early stage (radial growth phase) human melanoma cell lines: evidence for a dominant phenotype. Cancer Res 1996; 56: 3075-3086.
22) Livak KJ, Schmittgen TD. Analysis of relative gene expression data using real-time quantitative PCR and 2(-delta delta C(T)) method. Methods 2001; 25: 402-408.
23) Li YJ, Higgins RR, Pak BJ, Shivdasani RA, Ney PA, Archer M, Ben-David Y. p45NFE2 is a negative regulator of erythroid proliferation which contributes to the progression of friend virus-induced erythroleukemias. Mol Cell Biol 2001; 21: 73-80.
24) Wang X, Wang G, Shi Y, Sun L, Gorczynski R, Li Y-J, Xu Z, Spaner DE. PPAR-delta promotes survival of breast cancer cells in harsh metabolic conditions. Oncogenesis 2016; 5: e232.
25) Hall JM, Robinson ML. Peroxisome proliferator-activated receptor γ as a therapeutic target in human breast cancer. J Steroids Horm Sci 2015; 6: 155.

26) Du Y, Grandis JR. Receptor-type protein tyrosine phosphatases in cancer. Chin J Cancer 2015; 34: 61-69.

27) Whitmore TE, Peterson A, Holzman T, Eastham A, Amon L, McIntosh M, Ozinsky A, Nelson PS, Martin DB. Integrative analysis of N-linked human glycoproteomic data sets reveals PTPRF ectodomain as a novel plasma biomarker candidate for prostate cancer. J Proteome Res 2012; 11: 2653-2665.

28) Gearing KL, Gottlicher M, Teboul M, Widmark E, Gustafsson JA. Interaction of the peroxisome-proliferator-activated receptor and retinoid X receptor. Proc Natl Acad Sci U S A 1993; 90: 1440-1444.

29) Schmidt MV, Bruene B, von Knethen A. The nuclear hormone receoptor PPARγ as a therapeutic target in major diseases. ScientificWorldJournal 2010; 10: 2181-2197.

30) Aleshin S, Reiser G. Role of the peroxisome proliferator-activated receptors (PPAR)-alpha, beta/delta and gamma triad in the regulation of reactive oxygen species signaling in brain. Biol Chem 2013; 394: 1553-1570.

31) Juge-Aubry C, Pernin A, Favez T, Burger AG, Wahli W, Meier CA, Desvergne B. DNA binding properties of peroxisome proliferator-activated receptor subtypes on various natural peroxisome proliferator response elements. Importance of the 5'-flanking region. J Biol Chem 1997; 272: 25252-25259.

32) Hu E, Kim JB, Sarraf P, Spiegelman BM. Inhibition of adipogenesis through MAP kinase-mediated phosphorylation of PPARγ. Science 1996; 274: 2100-2103.

33) Eibl G, Wente MN, Reber HA, Hines OJ. Peroxisome proliferator-activated receptor gamma induces pancreatic cancer cell apoptosis. Biochem Biophys Res Commun 2001; 287: 522-529.

34) Blanquicett C, Roman J, Hart CM. Thiazolidinediones as anti-cancer agents. Cancer Ther 2008; 6: 25-34.

35) Tachibana K, Yamasaki D, Ishimoto K, Doi T. The role of PPARs in cancer. PPAR Res 2008; 2008: 102737.

36) Ostman A, Hellberg C, Bohmer FD. Protein-tyrosine phosphatases and cancer. Nat Rev Cancer 2006; 6: 307-320.

37) Brown-Shimer S, Johnson KA, Hill DE, Bruskin AM. Effect of protein tyrosine phosphatase 1B expression on transformation by the human neu oncogene. Cancer Res 1992; 52: 478-482.

38) Muller T, Choidas A, Reichmann E, Ullrich A. Phosphorylation and free pool of β-catenin are regulated by tyrosine kinases and tyrosine phosphatases during epithelial cell migration. J Biol Chem 1999; 274: 10173-10183.

39) Bera R, Chiou CY, Yu MC, Peng JM, He CR, Hsu CY, Huang HL, Ho UY, Lin SM, Lin YJ, Hsieh SY. Functional genomics identified a novel protein tyrosine phosphatase receptor type f-mediated growth inhibition in hepatocarcinogenesis. Hepatology 2014; 59: 2238-2250.

40) Laczmanska I, Karpinski P, Bebenek M, Sedziak T, Ramsey D, Szmida E and Sasiadek MM. Protein tyrosine phosphatase receptor-like genes are frequently hypermethylated in sporadic colorectal cancer. J Hum Genet 2013; 58: 11-15.

41) Phillips JM, Goodman JI. Identification of genes that may play critical roles in phenobarbital (PB)-induced liver tumorigenesis due to altered DNA methylation. Toxicol Sci 2008; 104: 86-99.